Absolute Equation of State Measurements on Shocked Liquid Deuterium up to 200 GPa (2 Mbar)

L. B. Da Silva, P. Celliers, G. W. Collins, K. S. Budil, N. C. Holmes, T. W. Barbee Jr., B. A. Hammel, J. D. Kilkenny, R. J. Wallace, M. Ross, and R. Cauble
Lawrence Livermore Laboratory, Livermore, California 94550

A. Ng and G. Chiu
University of British Columbia, Vancouver, British Columbia, Canada
(Received 13 August 1996)

We present results of the first measurements of density, shock speed, and particle speed in liquid deuterium compressed by laser-generated shock waves to pressures from 25 to 210 Gpa (0.25 to 2.1 Mbar). The data show a significant increase in D_2 compressibility above 50 Gpa compared to a widely used equation of state model. The data strongly suggest a thermal molecular dissociation transition of the diatomic fluid into a monatomic phase. [S0031-9007(96)02165-5]

PACS numbers: 62.50.+p, 64.30.+t, 64.70.–p

The equations of state (EOS) of hydrogen and its isotopes at high pressure are essential components of the physics of high density matter [1,2]. For example, the internal structure of Jovian planets is very sensitive to, and largely determined by, the hydrogen EOS in the 100–1000 Gpa (1–10 Mbar) pressure range [3]. In addition, the performance of deuterated inertial confinement fusion capsules relies on shock timing and efficient compression which are critically dependent on the EOS [4]. For these reasons a number of theoretical models of the EOS of hydrogen have been proposed [5–7]. An important outstanding question in the EOS of H_2, as well as D_2, has been the transition from a diatomic to a monatomic fluid. A continuous dissociative transition has been suspected, but theoretical predictions of molecular dissociation have been complicated by the presence of electronic transitions and possible ionization near pressures required for dissociation ($\sim$100 GPa) [8]. In spite of the expected simplicity of the element, there is no inclusive theory for a strongly coupled mixture of hydrogen ions, atoms, and molecules. In this Letter, we present results of the first measurements of the principal Hugoniot of liquid deuterium compressed up to pressures of 210 Gpa. These absolute EOS data reveal a substantially enhanced compressibility that is an indicator of dissociation.

EOS data for hydrogen in the pressure regime greater than 10 GPa have been obtained by both dynamic shock compression and static compression in diamond anvil cells. The latter method is used to study properties of solid hydrogen up to 250 GPa near room temperature [9]. Shock compression reaches higher temperatures, where the most accurate data have been produced using light gas guns [10,11]. While both methods access equilibrium states of matter, the final state densities and temperatures obtained by shock compression are directly applicable to inertial confinement fusion.

In shock compression, a single shock drives the fluid to a point on the principal Hugoniot, which is the locus of all final states of pressure, energy, and density that can be achieved behind a single shock wave passing through a material from an initial state. Conservation relations require that two independent parameters be measured to obtain an absolute EOS data point. (Comparative data are used to assess the EOS of one material with respect to another.) The shock speed U_s, the particle (or pusher) speed U_p, the pressure P, and the final density ρ are related by

$$P - P_0 = \rho_0 U_s U_p \tag{1}$$

and

$$\rho/\rho_0 = U_s/(U_s - U_p)\,, \tag{2}$$

where ρ_0 is the initial density, P_0 is the initial pressure and ρ/ρ_0 is the compression [12].

Early EOS experiments on H_2 and D_2 [10] were well described by a model using an intermolecular potential neglecting molecular dissociation [6]. However, recent temperature measurements revealed a significantly lower temperature than predicted for pressures larger than 20 GPa [11]. This was interpreted as dissocation of the molecular fluid at high density and temperature since dissociation removes energy from the liquid. A new model, referred to below as the dissociation model, was formulated to incorporate this effect [11]. The dissociation model is not an *ab initio* theory; it is based on the ideal mixing of molecular states (using a soft-sphere perturbation theory) and monatomic states (using a one-component plasma model), and includes a single adjustable parameter set to agree with all shock wave EOS and shock temperature data for H_2 and D_2 [10,11,13]. The inclusion of molecular dissociation leads to a significantly higher predicted compressibility in the 20–500 GPa regime. The density of D_2 on the Hugoniot at 100 GPa is 50% greater than calculated from both the earlier model [6] and the D_2 table included in the widely used Sesame EOS library [14].

The properties of deuterium shocked to high pressures by a high intensity laser have been examined previously, but the EOS of the material was not determined [15]. In order to obtain absolute EOS data, liquid D_2 was compressed with a Nova-laser-driven shock wave launched from an aluminum pusher. By following the propagation of the Al/D_2 interface and the shock front in the D_2 using temporally resolved radiography, measurements of the pusher speed, shock speed, and compression were obtained. The pressure is then determined by (1).

A schematic of the cryogenic target cell is shown in Fig. 1. Liquid D_2 was contained in a 1 mm diam, 0.45 mm long cylindrical cell machined into a copper block. One end of the cell was sealed with a 1100 alloy Al disk that served as the shock pusher; the opposite end of the cell was sealed with a 0.5 mm thick sapphire window. The pusher was 100, 180, or 250 μm thick, depending on the experiment, and had a rear-side mean surface roughness of 30 nm rms. The pusher was coated with 15–25 μm of polystyrene external to the cell; the polystyrene was then overcoated with a 100 nm layer of Al. The polystyrene layer thickness was chosen to prevent direct laser ablation of the Al pusher, minimizing x-ray emission and the consequent preheat of the pusher from x rays produced in the plasma. The Al overcoating eliminated direct optical laser shine through the plastic at the onset of the laser pulse. To accommodate radiography through the sides of the cell, a 500 μm diam window was drilled into each side of the cell and sealed with a 5 μm thick beryllium foil.

Liquid D_2 (99.98% pure) was loaded into the cell at 19.4–19.8 K and then pressurized to a few hundred Torr. Temperatures were monitored to within 0.05 K. D_2 densities were determined from the saturation curve [16] and varied between 0.170 and 0.172 g/cm^3. The initial density ρ_0 for each experiment was known with an uncertainty of less than 0.1%.

One beam of the Nova laser ($\lambda = 527$ nm) was focused onto the target. Ablation of the polystyrene layer drove a shock wave through the Al and into the D_2. Side-on radiography of the D_2 revealed propagation of the Al/D_2 interface and the shock front. To ensure a spatially planar and uniform shock front, a phase plate was inserted into the Nova beam to generate a smooth laser irradiance profile. The laser spot at the target plane was elliptical with major and minor diameters up to 900 and 600 μm, respectively, depending on focusing. Drive irradiances ranged from 5×10^{12} to 2×10^{14} W/cm^2. The Nova drive beam had an 8 or 10 ns temporally square profile with a rise time of 100 ps.

The results of the measurement depend on knowing the initial state of the D_2, i.e., ρ_0, prior to shock arrival. This made it necessary to determine the preheat level of the pusher/D_2 interface at the time the shock arrives. The position of the rear pusher surface was monitored with a Michelson interferometer through the sapphire window [17]. This provided the additional advantage of verifying the planarity of the shock at breakout. The interferometer probe beam was a 10 ns FWHM, 355 nm laser pulse appropriately time delayed from the Nova drive beam which generated the shock wave. The experimental arrangement is shown in Fig. 2.

Results of the interferometry showed substantial expansion of the rear of the aluminum pusher prior to shock breakout when no plastic ablation layer was used on the front side. There was also some slight expansion when a plastic-coated, 100 μm thick pusher was driven at the highest intensity; the rear side expanded by approximately 0.3 μm. Even for the long pulses used here, interferograms of the thicker pushers (180 and 250 μm) exhibited no rear surface motion. Given the detection limit of 0.2 fringe, which corresponds to movement of 30 nm at the pusher surface, we estimate that the maximum pusher surface temperature prior to shock breakout was ~400 K, negligible in this experiment. The interference fringes disappear due to absorption of the probe light as the shock emerges from the Al/D_2 interface. Since the interferometer is spatially resolved in one dimension, we observed that at breakout the shock front was uniform and planar to within ± 2.5 μm over a lateral region of 350 μm.

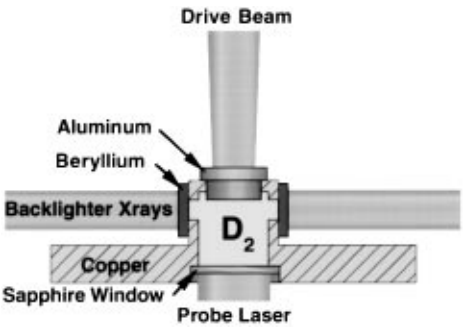

FIG. 1. Schematic diagram of the cryogenic cell for laser-driven shock compression of liquid deuterium.

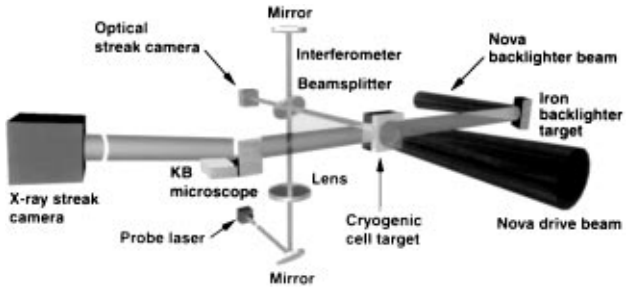

FIG. 2. Schematic diagram of the experimental setup for simultaneous side-on radiography and end-on interferometry of the cryogenic cell including three laser beams: one smoothed Nova beam to drive a shock in the cell, an oppositely directed Nova beam to provide an x-ray backlighter, and a third beam for the interferometer.

Streaked radiography o the shocked D_2 was performed using a plasma x-ray source produced by focusing a second beam of Nova onto a Fe disk (10 ns at 6×10^{13} W/cm^2). The backlighter was placed 12 cm away from the target cell to eliminate heating of the cell and to produce a near-collimated x-ray source. The effective source size in the imaging direction was approximately 150 μm and was set by the laser focal spot width. Using the interferometer, the x-ray backlighter was observed to have no affect on the D_2 in the cell. X rays transmitted through the target cell were imaged by a Kirkpatrick-Baez microscope (K-B) onto a streak camera. The K-B bandpass was 750–840 eV and the collection half-angle was 2.5 mrad. Two different calibrated magnifications were used, 33× and 82×. The resolution of the K-B microscope in this geometry was found to be better than 3 μm over a 300 μm wide field of view. The microscope imaged a strip 300 μm long by 5–30 μm wide, depending of magnification and configuration.

An example of a streaked radiograph of shock-compressed D_2 is shown in Fig. 3. The drive irradiance was 10^{14} W/cm^2 over 8 ns. The bright area is the view through the side windows of the cell. Since the pusher is opaque and the liquid transparent, the Al/D_2 interface is the boundary between the light and dark regions. In the figure, the interface is stationary prior to 2 ns. At 2 ns the laser-driven shock crosses the interface and the pusher surface accelerates to a steady speed, the particle speed. As the shock wave is driven into the D_2, a shock front can be seen moving ahead of the interface. The shock front, which appears as the dark line, is made visible because of refraction of backlighter x rays at the density jump across the shock front. X rays grazing the shock front interface are refracted to angular deflections greater than 2.5 mrad and therefore out of the angular field of the K-B. (X rays impinging at nongrazing angles are internally reflected, which is why there is transmission between the Al/D_2 interface and the shock front.) This is similar to the Schlieren technique for detecting density gradients. The steady propagation of both the shock front and the interface is demonstrated by their linear trajectories until ~6 ns when a stronger shock enters the D_2. The second shock is caused by shock reverberations in the pusher. (In this example, no data after 6 ns were used.) The shock and particle speeds, U_s and U_p, can be evaluated from the slopes.

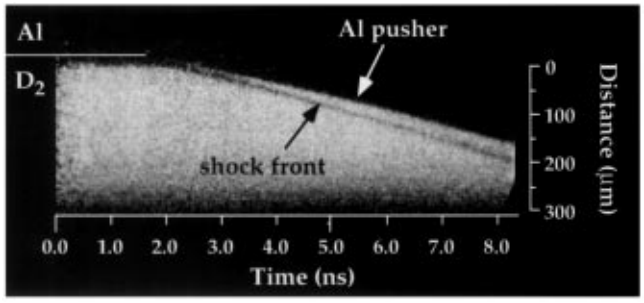

FIG. 3. A time-resolved side-on radiograph of a laser-shocked D_2 cell. The bright area views the D_2 through beryllium windows bounded by the x-ray-opaque aluminum pusher above. The pusher is seen advancing after breakout at 2 ns; the shock is the dark line in front of, and moving faster than, the pusher/D_2 interface.

The single shock compression can be determined by (2) using the individually derived shock and pusher speeds, but it can be measured directly from the film as long as U_s and U_p are constant. (In the experiments, U_s and U_p are constant to better than 1%.) At any time t, the compression is equal to the ratio of two lengths: the distance between the shock front $X_s(t)$ and the initial interface position X_0, the thickness of a layer of uncompressed D_2, and the distance between the shock front and the interface $X_l(t)$, which is the thickness of the now-compressed layer. Thus $\rho/\rho_0 = [X_s(t) - X_0)/(X_s(t) - X_l(t)]$. Since all of the measurements are made on one piece of film in the streak camera, uncertainties in magnification and sweep speed cancel in this ratio. In the experiments, a steady shock was observed for 4–8 ns with no measurable change in speed of the Al/D_2 interface. Comparison with (2) provides an internal consistency check on ρ/ρ_0.

The shock position that we observe in the radiograph is the leading part of the shock front which emerges from the center of the pusher. In some experiments, the apparent Al/D_2 interface position at $t = 0$ on film was not identical to the actual value of X_0 due to the fact that the rotation of the cell about the axis perpendicular to both the backlighter path and the shock path (the axis looking into the page in Fig. 1) could be controlled only to within 3 mrad. This resulted in the center of the pusher being shadowed by an edge of the pusher before the shock front emerged from the pusher. In these cases, the shock and interface trajectories did not converge on the film. However, extrapolation of the trajectories revealed X_0 as the intersection of the two paths. Alternatively, shock and interface positions taken at two at different times could be used to determine X_0. This resulted in a correction of as much as 10% to the compression obtained using the *apparent* position X_0 on film and increased the uncertainty in ρ/ρ_0 from about ±3% to ±5%.

The Al/D_2 interface is subject to the Richtmyer-Meshkov hydrodynamic instability (RM). However, using the measured pusher finish of 30 nm, we calculate that the largest perturbation expected from RM is less than 0.5 μm during the times of observation, of the order of 1–2% of the compression.

Figure 4(a) shows the measured shock speeds and final densities determined from the known initial densities and measured compressions. As explained above, the error bars are governed predominantly by the accuracy in determining the slopes of the shock and interface trajectories in the radiographs. The figure plots Hugoniots from the dissociation model [11] and the Sesame EOS table [14].

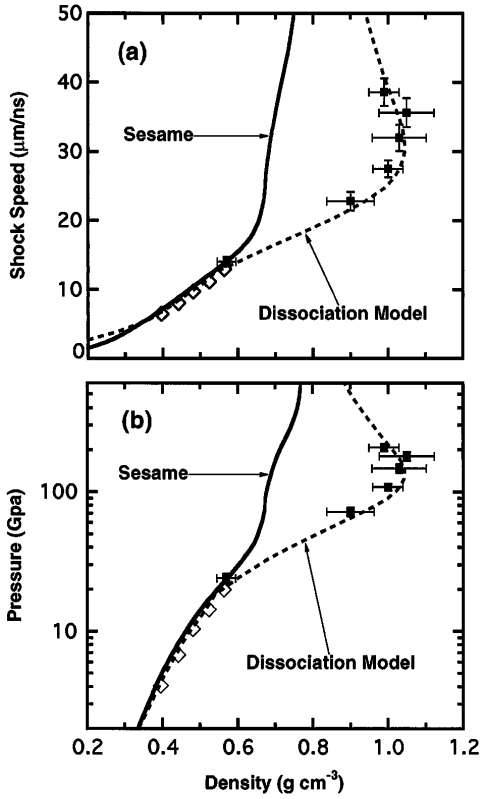

FIG. 4. (a) The measured data are shown as squares with error bars compared with Hugoniots derived from the Sesame EOS library [14], which is similar to an EOS without dissociation [6], and the proposed dissociation model of Ref. [11]. The diamonds are gas gun data [10]. (b) The data are presented as pressure vs density.

The gas gun observations [10] are shown as well. At the lowest compression, our data are in agreement with the earlier results, while at higher compressions the data deviate from the Sesame prediction. Figure 4(b) shows the pressure determined from (1). Our datum at 25 GPa is significant because it overlies the more accurate gas gun data, lending confidence to our results. The laser data evince an enhanced compressibility comparable to that of the dissociation model in the region where strong dissociation is predicted to occur. We conclude from this that molecular dissociation is indeed significant in hydrogen isotopes compressed near 100 GPa.

In conclusion, we have presented the first measurement of the density, shock speed, and particle speed in deuterium at pressures from 25 to 210 GPa. These absolute Hugoniot data strongly indicate a dissociative transition from the diatomic to the monatomic fluid state and provide an important benchmark for a revised equation of state model for hydrogen and its isotopes in a regime relevant to high energy density physics. Additionally, the experiments demonstrate that laser-driven shock waves can effectively be used for equation of state studies at pressures beyond those attainable by traditional techniques.

The authors would like to thank S. Dixit for the phase plate, D. A. Young, F. J. Rogers, and R. M. More for useful discussions on the theory, S. G. Glendinning for help with image processing, T. Weiland for assistance with the interferometer laser, W. Unites, R. Jones, J. Burman, S. Letts, E. Mapoles, J. Pipes, and J. Sanchez for assembly of the cryostate and cells, J. Cox and K. Haney for diagnostic development, J. Cardinal and D. Cocherell for diagnostic design and installation, the Nova target fabrication group, and the Nova operations technical support personnel. A. N. and G. C. acknowledge the support of the Natural Sciences and Engineering Research Council of Canada. This work was performed by Lawrence Livermore National Laboratory under the auspices of the U.S. Department of Energy under Contract No. W-7405-ENG-48.

[1] S. Ichimaru, H. Iyetomi, and S. Tanaka, Phys. Rep. **149**, 91 (1987).
[2] N. W. Ashcroft, Phys. World **8**, (7) 43 (1995).
[3] R. Smoluchowski, Nature (London) **215**, 691 (1967); V. N. Zharkov and V. P. Trubitsyn, in *Jupiter*, edited by T. Gehrels (University of Arizona Press, Tucson, 1976), pp. 135–175.; W. B. Hubbard, Science **214**, 145 (1981); D. J. Stevenson, Annu. Rev. Earth Planet. Sci. **10**, 257 (1982); W. J. Nellis, M. Ross, and N. C. Holmes, Science **269**, 1249 (1995).
[4] J. D. Lindl, Phys. Plasmas **2**, 3933 (1995).
[5] W. B. Hubbard, Astrophys. J. **152**, 745 (1968).
[6] M. Ross, F. H. Ree, and D. A. Young, J. Chem. Phys. **79**, 1487 (1983).
[7] D. Saumon, G. Chabrier, and H. M. Van Horn, Astrophys. J. Suppl. **99**, 713 (1995).
[8] W. R. Magro, D. M. Ceperley, C. Pierleoni, and B. Bernu, Phys. Rev. Lett. **76**, 1240 (1996).
[9] H. K. Mao and R. J. Hemley, Rev. Mod. Phys. **66**, 671 (1994).
[10] W. J. Nellis, A. C. Mitchell, M. van Theil, G. J. Devine, R. J. Trainor, and N. Brown, J. Chem. Phys. **79**, 1480 (1983).
[11] N. C. Holmes, M. Ross, and W. J. Nellis, Phys. Rev. B **52**, 15 835 (1995).
[12] Y. B. Zel'dovich and Y. P. Raizer, *Physics of Shock Waves and High-Temperature Hydrodynamic Phenomena* (Academic Press, New York, 1966).
[13] S. T. Weir, A. C. Mitchell, and W. J. Nellis, Phys. Rev. Lett. **76**, 1860 (1996).
[14] G. I. Kerley, Los Alamos Scientific Laboratory Report No. LA-4776, 1972 (unpublished).
[15] C. G. M. van Kessel and R. Sigel, Phys. Rev. Lett. **33**, 1020 (1974); K. A. Tanaka *et al.*, in *Shock Waves*, edited by K. Takayama (Springer-Verlag, Berlin, 1992), p. 863.
[16] P. C. Souers, *Hydrogen Properties for Fusion Energy* (University of California Press, Berkeley, 1986).
[17] K. S. Budil *et al.*, Characterization of preheat in Laser-Driven Targets using Interferometry, American Physical Society Division of Plasma Physics Conference, 1996 (to be published).